Science Advances
AAAS

advances.sciencemag.org/cgi/content/full/5/8/eaaw2398/DC1

Supplementary Materials for

Bulk ultrafine grained/nanocrystalline metals via slow cooling

Chezheng Cao, Gongcheng Yao, Lin Jiang, Maximilian Sokoluk, Xin Wang, Jim Ciston, Abdolreza Javadi, Zeyi Guan, Igor De Rosa, Weiguo Xie, Enrique J. Lavernia, Julie M. Schoenung, Xiaochun Li*

*Corresponding author. Email: xcli@seas.ucla.edu

Published 23 August 2019, *Sci. Adv.* **5**, eaaw2398 (2019)
DOI: 10.1126/sciadv.aaw2398

This PDF file includes:

Supplementary Text
Fig. S1. Fabrication of Cu-containing WC nanoparticles.
Fig. S2. Cooling curves for furnace cooling, air cooling, and water quenching of Cu-WC samples.
Fig. S3. Size distribution of WC nanoparticles in the as-solidified Cu-WC sample.
Fig. S4. Structure of bulk UFG/nanocrystalline Cu-containing WC nanoparticles.
Fig. S5. STEM image of the WC nanoparticle-rich area showing that the Cu grain size is correlated with WC interparticle spacing.
Fig. S6. Cooling curve during the DSC tests at a cooling rate of 5°C/min.
Fig. S7. Mechanical properties of UFG/nanocrystalline Cu-containing WC nanoparticles.
Fig. S8. Undercooling profile relative to solid fraction.
References (*39*–*45*)

Supplementary Text

Nanoparticle dispersion and self-stabilization mechanism

Prior studies reported silicon carbide nanoparticles could be dispersed in magnesium matrix by a self-dispersion and self-stabilization mechanism *(36)*. There are three major factors contributing in this theory: (1) Good wetting between molten metal and nanoparticles creates an energy barrier to prevent atomic contact and sintering of nanoparticles in the melt. In our Cu-WC system, the energy barrier can be calculated by the following equation

$$W_{barrier} = S\sigma_{Cu}\cos\theta$$

where S is the effective area and can be calculated by $S=\pi RD_0$ (D_0=0.2 nm), σ_{Cu} is the surface energy of Cu at the processing temperature (about 1.27 J m^{-2}) *(40)*, and θ is the wetting angle, e.g. at 1250 °C (10°) *(29)*. In the Cu-WC system, an energy barrier of 7×10^4 zJ is obtained; (2) Thermal energy that enable nanoparticles to move randomly in the molten melt by overcoming the attractive van der Waals potential between nanoparticles. A higher thermal energy is preferred. The processing temperature for Cu-WC is 1250 °C, which provide a thermal energy of $E=k_bT$=21.0 zJ. (3) A van der Waals potential between nanoparticles to lessen the attraction of nanoparticles from each other to form nanoparticles clusters in molten metals. A small attractive van der Waals potential is preferred. It can be calculated by the following equation *(41)*

$$W_{vdw} = -\frac{(\sqrt{A_{Cu}} - \sqrt{A_{WC}})^2}{6D}\frac{R}{2}$$

where A_{Cu} = 410 zJ and A_{WC} are the Hamaker constants, D is the distance between two nanoparticles that can be as small as two atomic layer thick (0.4 nm), R is the radius of the nanoparticle (100 nm). Although the data of A_{wc} is not available, a 7×10^4 zJ energy barrier is several orders of magnitude higher than thermal energy. Since WC is conductive ceramic material, A_{wc} is estimated to be in the range of 200 to 500 zJ *(41)*, suggesting that $W_{barrier}$ would always be much higher than W_{vdw} for stabilization of dispersed WC nanoparticles in Cu melt.

Growth restriction factor by nanoparticles

For growth restriction by extra solute atoms, the constitutional undercooling could be described by *(17)*

$$\Delta Tc = mC_0(1 - \frac{1}{(1-f_s)^{(1-k)}})$$

where ΔT_c is the constitutional undercooling, m is the liquidus slope in a linear phase diagram, C_0 is the solute content in the alloy and k is the equilibrium solute partition coefficient, f_s is the solid fraction solidified. By taking the derivative of this equation respect to f_s, it has been suggested that Q can be expressed as *(9, 17)*

$$Q = mC_0(k-1) = (\frac{\partial(\Delta T_c)}{\partial f_s})_{fs\to0}$$

This equation indicates that the physical meaning of growth restriction factor is the initial rate of development of constitutional undercooling. Taking Al-Ti as one example, the constitutional undercooling of Al-Ti alloy system is shown in fig. S8. Ti is the one of the most effective atoms to restrict grain growth in Al. The growth restriction factor is described as Q_1, Q_2 and Q_3 for different Ti concentration of 0.05, 0.10 and 0.15, respectively. With higher concentration of Ti atoms in Al melt, the growth restriction factor increases. As marked by the black arrow in the fig. S8, a steeper slope provides larger growth restriction factor. However, the maximum solubility of Ti atoms in Al is 0.15 which limits Q to reach a maximum value as Q_{max} .
In contrast, the new growth restriction factor, Q_{np}, introduced by nanoparticles enabled phase control break the fundamental limit set by Q that depends on constitutional undercooling. As far as the solidification front touches with a nanoparticle with curved shape or a nano-scale channel between nanoparticles, unlike the constitutional undercooling built gradually ahead of the solidification front, an undercooling is immediately established by the Gibbs-Thompson effect. As shown in fig. S8, the undercooling profile established by Gibbs-Thompson effect is a step function with an infinite large slope at the initial point. Thus Q_{np} which is the initial rate of the undercooling development by nanoparticles can be readily increased to a significant large number, if not infinity.

Strengthening mechanism

The strengthening from nanoparticles and refined grain structures in the as solidified samples of Cu-34vol%WC is about 647 MPa. The major strengthening mechanisms include Orowan strengthening induced from the populous and dispersed nanoparticles, Hall-Petch effect, and load bearing transfer.
The contribution from Orowan strengthening ($\Delta\sigma_{Orowan}$) from well-dispersed nanoparticles can be calculated by the following equation *(42, 43)*

$$\Delta\sigma_{Orowan} = \frac{0.13 G_m b}{d_p\left[\left(\frac{1}{2V_p}\right)^{\frac{1}{3}} - 1\right]} ln\frac{d_p}{2b}$$

where G_m, b, V_p and d_p are the shear modulus of the matrix, the Burger vector, the volume fraction and the size of the nanoparticles, respectively. In this study, G_m= 46 GPa, b = 0.256 nm, V_p = 0.34 and d_p = 200 nm, the calculated $\Delta\sigma_{Orowan}$ is 333 MPa. It should be noted that this value is estimated based on ideal dispersion.
The contribution from Hall-Petch effect can be calculated by the following equation *(44)*

$$\Delta\sigma_y = kd^{-1/2}$$

where d is the grain size and k is a material constant. For Cu, k = 0.11 MPa·m, and d = 208 nm, the calculated $\Delta\sigma_y$ = 246 MPa.
The load bearing strengthening can be calculated by the following equation *(45)*

$$\Delta\sigma_{load} = 1.5 V_p \sigma_i$$

where σ_i is the interfacial bonding strength between nanoparticles and metal matrix. The strong interfacial bonding between Cu and WC nanoparticles contributes in the load bearing mechanism. It is difficult to estimate the interfacial bonding strength though.

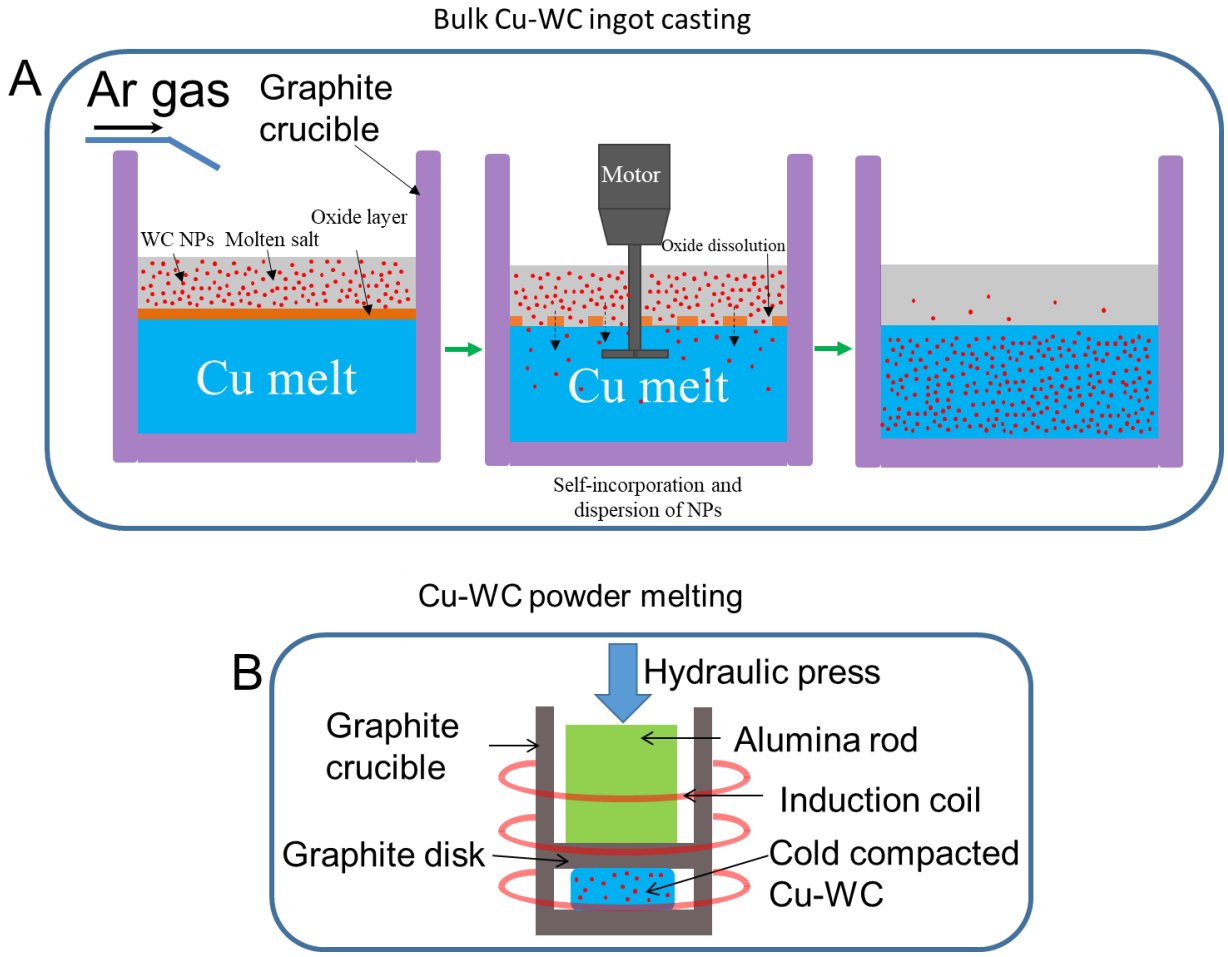

Fig. S1. Fabrication of Cu-containing WC nanoparticles. (**A**) Schematic illustration of the salt-assisted self-incorporation for Cu-WC before casting bulk ingots. (**B**) Schematic illustration of the powder melting method to cast Cu containing WC nanoparticles.

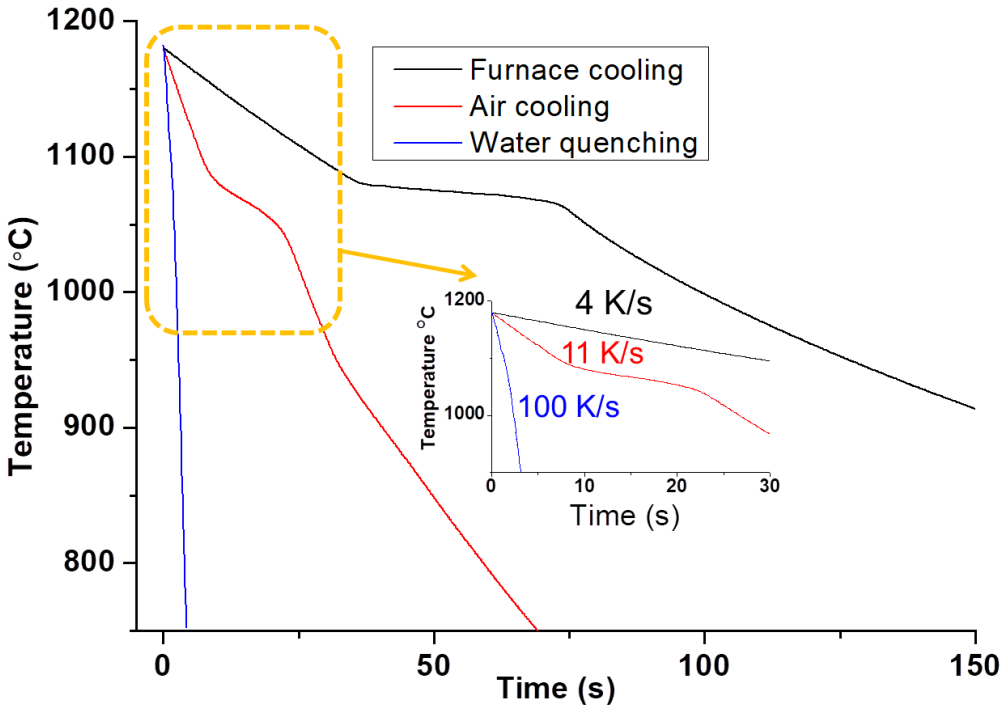

Fig. S2. Cooling curves for furnace cooling, air cooling, and water quenching of Cu-WC samples.

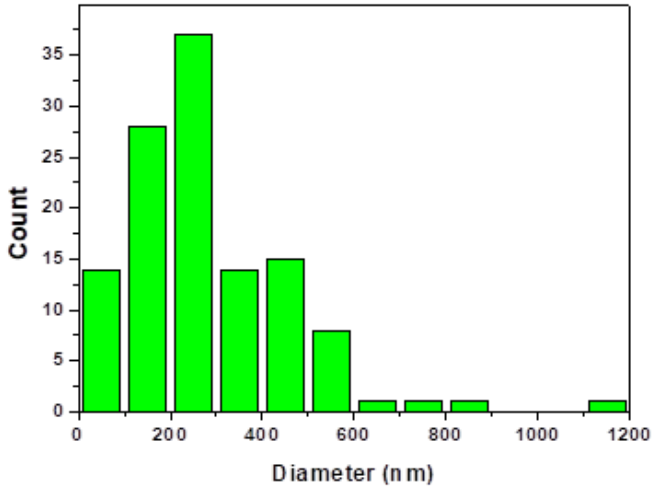

Fig. S3. Size distribution of WC nanoparticles in the as-solidified Cu-WC sample.

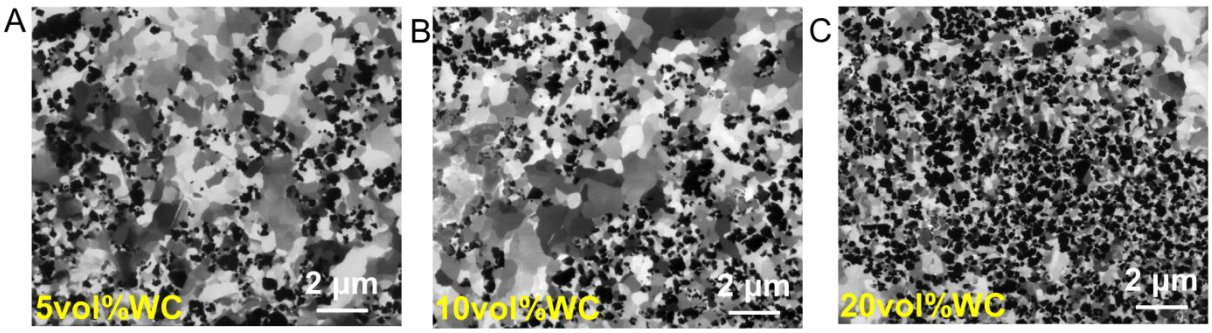

Fig. S4. Structure of bulk UFG/nanocrystalline Cu-containing WC nanoparticles. (**A-C**) FIB image of Cu-5vol%WC, Cu-10vol%WC and Cu-20vol%WC, respectively.

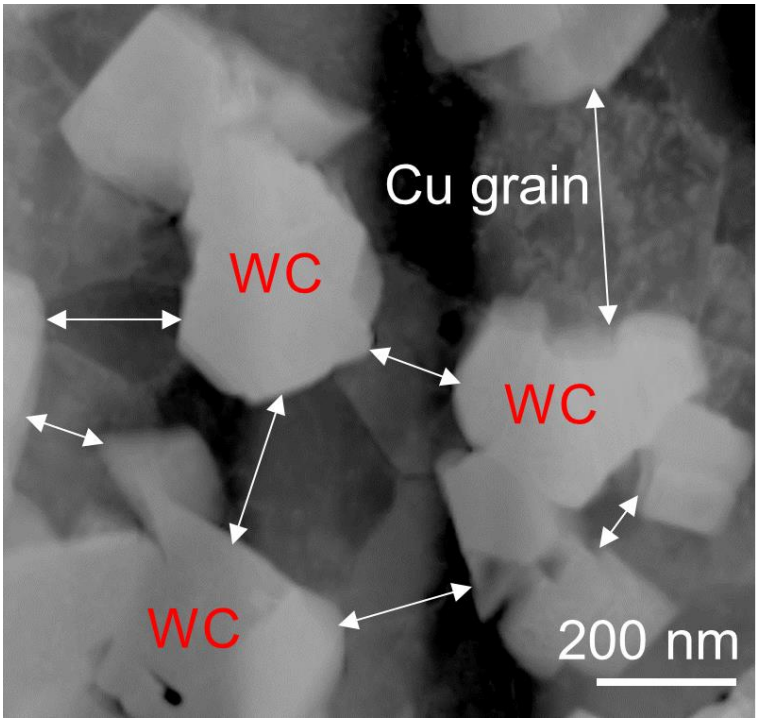

Fig. S5. STEM image of the WC nanoparticle-rich area showing that the Cu grain size is correlated with WC interparticle spacing.

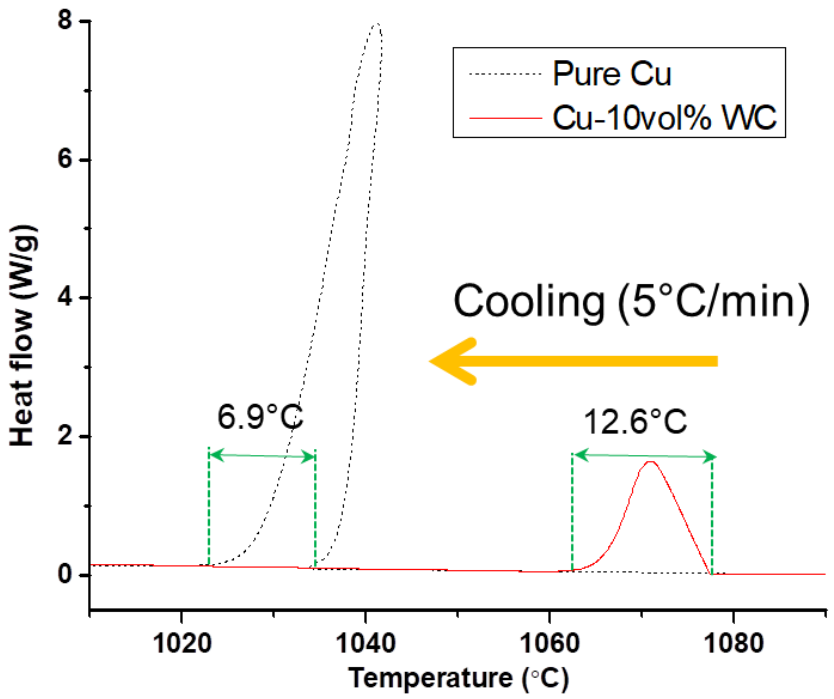

Fig. S6. Cooling curve during the DSC tests at a cooling rate of 5°C/min.

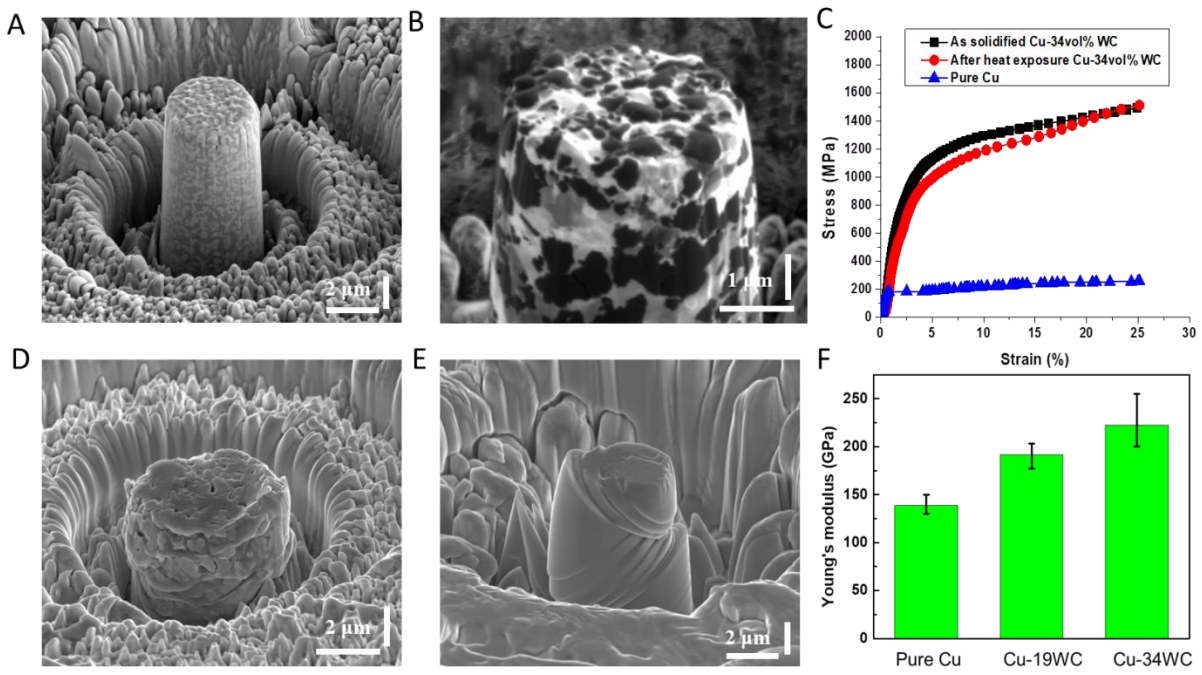

Fig. S7. Mechanical properties of UFG/nanocrystalline Cu-containing WC nanoparticles. (**A**) SEM image of a Cu-34vol%WC micropillar machined by FIB. (**B**) FIB image of the micropillar showing polycrystalline Cu matrix with WC nanoparticles. (**C**) Engineering stress-strain curves of as-solidified pure Cu samples (blue), with nanoparticles (black) and heat treated sample (red). (**D-E**) SEM images showing the morphology of post-deformed samples with (D) and without (E) nanoparticles. (**F**) Young's modulus of pure Cu, Cu-19vol%WC and Cu-34vol%WC.

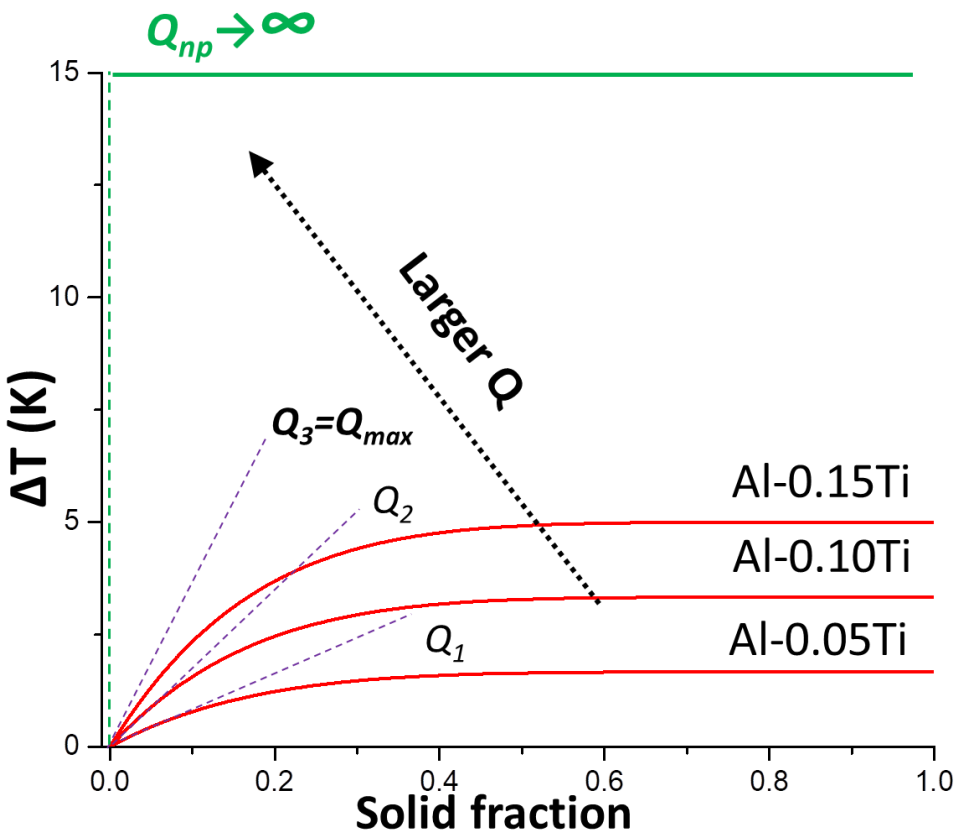

Fig. S8. Undercooling profile relative to solid fraction. The red curves correspond with the constitutional undercooling for Al-Ti alloys. Limited by the phase diagram and the maximum solubility of Ti in Al, the growth restriction factor reaches to a maximum value of Q_{max} in the Al-0.15Ti alloy. However, the undercooling profile of the nanoparticle enabled phase growth restriction indicates an almost infinity large Q_{np}.